Journal of Building Engineering 92 (2024) 109815

Contents lists available at ScienceDirect

Journal of Building Engineering

journal homepage: www.elsevier.com/locate/jobe

Improving the early-age behavior of concrete containing coarse recycled aggregate with raw-crushed wind-turbine blade

Daniel Trento [a,b], Flora Faleschini [a], Víctor Revilla-Cuesta [b], Vanesa Ortega-López [b,*]

[a] Department of Civil, Environmental and Architectural Engineering, University of Padova, Via Francesco Marzolo 9, 35131, Padova, Italy
[b] Department of Civil Engineering, Escuela Politécnica Superior, University of Burgos, c/ Villadiego s/n, 09001, Burgos, Spain

ARTICLE INFO

Keywords:
Recycled aggregate
Wind-turbine blade
Concrete
Concrete curing
Plastic shrinkage
Flexural strength

ABSTRACT

Recycled aggregate used in replacement of coarse natural aggregate can lower the quality of both fresh and hardened concrete properties. There are many methods to reduce the negative effects of recycled aggregate in the literature, although most involve unsustainable solutions that jeopardize any environmental benefits associated with their use. In this study, a novel approach is presented for mitigating the adverse impacts of coarse recycled aggregate used in concrete mixes. Furthermore, it allows solving the current issue of the recycling of wind-turbine blades at the same time. Raw-crushed wind-turbine blade, a waste from the crushing of decommissioned wind-turbine blades with a high proportion of glass fiber-reinforced polymer fibers, was added to concrete mixes containing coarse recycled aggregate. As a main outcome, additions of that waste were found to enhance the early-age properties of concrete containing that kind of aggregate. Plastic shrinkage was reduced, and flexural strength increased by as much as 47 % and 14 %, respectively, while compressive strength remained approximately constant.

1. Introduction

Usage of cementitious concrete that is manufactured in larger amounts than any other construction material in the world [1,2] is only expected to increase, in response to the exponential rate of global population growth. Up to 80 % of total concrete volume can consist of sand and gravel [2,3], so the exploitation of quarries and gravel pits is therefore also set to increase over upcoming years. On the one hand, the demand for aggregate within the construction sector has been steadily growing at a rate of around 5.2 % *per* year, resulting in consumption, for example, of a total of 51.79 billion tons in 2019 [4]. On the other hand, the production of Construction and Demolition Waste (C&DW) has also been increasing [3,5], disposal of which is still a problem in many countries, as around 35 % of all C&DW is landfilled [6]. The replacement of conventional aggregate with recycled aggregate from C&DW is the most widespread and well-known solution, both for the reduction of natural-aggregate consumption and for the recovery and reuse of C&DW [7].

Despite its environmental advantages, the use of recycled aggregate in replacement of conventional aggregate is still limited, due to the inferior performance of the resulting concrete [8]. This worsening of performance caused by recycled aggregate can be found at all concrete ages [4]. However, it is more noticeable at early ages because recycled aggregate delays concrete strength development [5,7]. Furthermore, its high flexibility compromises concrete stiffness to a greater extent because the development of stiffness by the cementitious matrix is still in progress [4]. This leads not only to a reduction in mechanical properties, but also to increased plastic shrinkage that favors the appearance of cracks and weakens the durability behavior of concrete [8].

* Corresponding author.
E-mail address: vortega@ubu.es (V. Ortega-López).

https://doi.org/10.1016/j.jobe.2024.109815
Received 3 May 2024; Received in revised form 27 May 2024; Accepted 1 June 2024
Available online 1 June 2024

Nevertheless, significant improvements to the properties of Recycled Aggregate Concrete (RAC) can be achieved through several methods. Such strategies include the removal or strengthening of adhered mortar in the recycled aggregate [9–12], the addition of supplementary cementitious materials [13,14], and particularly the incorporation of fibers, which offers numerous advantages for RAC [15–17]. One key benefit of fiber additions is the significant improvement of RAC tensile properties, which are otherwise usually low due to weak bonding between the cementitious matrix and this type of aggregate [18]. Fibers also effectively limit the formation and propagation of micro-cracks, which in turn contributes to enhanced durability of RAC [19,20]. Additionally, the presence of recycled aggregate and, therefore, mortar fragments, favors the development of shrinkage cracks, whose formation and propagation can be controlled through the addition of fibers, which serve as rigid elements restraining contraction within the cementitious matrix [18].

Glass Fiber-Reinforced Polymer (GFRP) is a composite material that comprises glass fibers embedded within polymeric epoxy resins. Its usage in the construction and the aerospace industry, and the energy sector has been spreading more than ever before over recent years, because of its superior mechanical properties [21]. In 2017, the demand for GFRP materials within the United States reached an annual total of almost 2 million tons [22]. Therefore, the current high production and consumption of GFRP materials is resulting in the generation of significant volumes of GFRP-composite waste [23].

In that context, the wind-energy sector is an important source of GFRP-composite waste production, as that material is the main component of wind-turbine blades [24]. In the wind farms of the United States, there are currently over 190,000 functional turbine blades that have been operating for at least 20 years, which is approximately the lifespan of conventional wind turbines [25], and approximately 235,000 blades will have been replaced before the end of 2050 [26]. The estimated accumulation of post-service blades is therefore expected to reach approximately 1.5 million tons by the year 2040 in the United States [26] and to rise to 2.1 million tons by 2050 [27]. In parallel, wind power currently satisfies 17 % of Europe's electricity needs and significantly surpasses that percentage in several nations [28]. Wind energy currently supplies 55 % of all electricity consumed in Denmark, while that figure is 34 % in Ireland, 28 % in the UK, 26 % in Portugal, 26 % in Germany, and 25 % in Spain. According to the International Energy Agency's projections, wind energy is anticipated to become Europe's primary electricity source by 2027 [28]. In Spain, approximately 1000 wind turbines underwent dismantling in 2023, with an expected maximum estimate of about 2500 wind turbines that will have to be dismantled *per* year by 2029 [24]. From that point, between 4500 and 6000 wind-turbine blades will be dismantled every year in Spain, which will result in 10,000 tons of blade waste annually [28]. These figures urgently require a solution for the recovery and the recycling of GFRP-composite waste.

Wind-turbine blades, aside from the metallic circular joint connecting them to the nacelle, primarily consist of a GFRP composite that offers suitable mechanical strength at the same time as adequate durability. Nevertheless, they are also composed of other materials. The inclusion of lightweight materials such as balsa wood and polymers sandwiched with GFRP enhance the bending strength of the blades and decrease their overall weight [29]. Additionally, a polymeric resin coating is applied to the blade surface, and polyvinyl chloride stiffeners may be employed in certain instances [30]. All these components are difficult to separate, which means that blade recycling is a challenging area of research. One way of recovering and recycling wind-turbine blades is the production of Raw-Crushed Wind-Turbine Blade (RCWTB). Its production involves the crushing of wind-turbine blades without having previously separated the individual components [31]. The resulting waste material consists of fibers made of GFRP composite mixed with roughly spherical particles of balsa wood and polymers [29].

In this work, RCWTB was added to concrete to limit the detrimental effects of Coarse Recycled Aggregate (CRA) in concrete manufacturing, an aspect that has not previously been studied in the scientific literature to the best of the authors' knowledge. The specific aim was to analyze whether RCWTB can improve the early-age behavior of RAC, mainly focusing on shrinkage, compressive strength and flexural strength under different curing conditions. The early-age behavior of concrete was evaluated since this is the age at which the negative effect of the recycled aggregate is most pronounced [4]. In that way, the aim was also to elucidate whether RCWTB can offer a better balance between those properties within CRA concrete at an early age.

2. Experimental program

2.1. Materials and components

CEM II/A-L 42.5 R cement as *per* BS EN 197-1 [32] was employed in this experimental campaign, which contains limestone as a

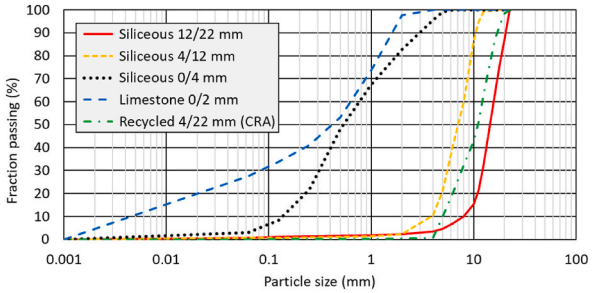

Fig. 1. Grading curves of the aggregates.

clinker replacement in percentages ranging between 6 and 20 %. Water from the mains supply network of Burgos was used. Two superplasticizer admixtures that showed optimal interaction were added to reach an adequate workability with a reduced water/-cement ratio: one consisted of a modified polycarboxylate with a water-base, while the second was composed of a modified polycarboxylate.

Five types of aggregates were considered to reach a suitable joint gradation, whose Saturated-Surface-Dry (SSD) density and 24-h Water Absorption (WA) were tested according to BS EN 1097-6 [32] and whose gradation curves are shown in Fig. 1. First, three siliceous aggregates, in fractions of 12/22 mm (SSD density of 2.60 kg/dm^3 and 24-h WA of 0.55 %), 4/12 mm (SSD density of 2.63 kg/dm^3 and 24-h WA of 0.33 %), and 0/4 mm (SSD density of 2.62 kg/dm^3 and 24-h WA of 0.13 %); second, a limestone sand 0/2 mm (SSD density of 2.66 kg/dm^3 and 24-h WA of 0.10 %); and a CRA 4/22 mm (SSD density of 2.44 kg/dm^3 and 24-h WA of 6.12 %). The CRA utilized in this research was obtained from the crushing of concrete elements produced with siliceous aggregate that had a characteristic compressive strength of 45 MPa. Supplied by a Spanish company specialized in C&DW, the CRA was more than 5 years old when it was used, so the shrinkage and strength development of its adhered mortar had already stabilized. It was carefully sieved and sorted in the laboratory to retain only the coarse fraction that ranged between 4-to-22 mm in size.

The RCWTB was prepared by crushing rectangular panels composed of GFRP composite, balsa wood, and polymeric layers. Those panels, measuring approximately 20–30 cm on each side, were crushed using a knife mill and then sieved to produce the RCWTB. The resulting RCWTB consisted of GFRP-composite fibers and spherical particles of balsa wood and polymers. The content of GFRP-composite fibers was 66.8 % by weight, measured through sieving and manual separation, the length and diameter of which were evaluated in multiple samples, yielding average values of 13.1 and 0.73 mm, respectively, resulting in a mean aspect ratio of around 18. The RCWTB had a density of 1.63 kg/dm^3, determined according to the standardized procedure for the aggregates (BS EN 1097-6 [32]). A previous work conducted by some of the authors provides a detailed characterization of RCWTB, in which a microstructural analysis of this waste can also be found [24].

Fig. 2 depicts the aggregates and the RCWTB used in the experimental campaign.

2.2. Mix design

Six concrete mixtures were cast in this research. Three of them were prepared as references with CRA amounts of 0 %, 50 %, and 100 %, without employing RCWTB. The other three incorporated 6 % RCWTB over the total volume of the aggregates. The key aspects of the mix design were as follows:

- The amount of RCWTB was fixed at 6 % of the aggregate volume as, according to a previous work [29], the flexural strength of conventional concrete increased at that content.

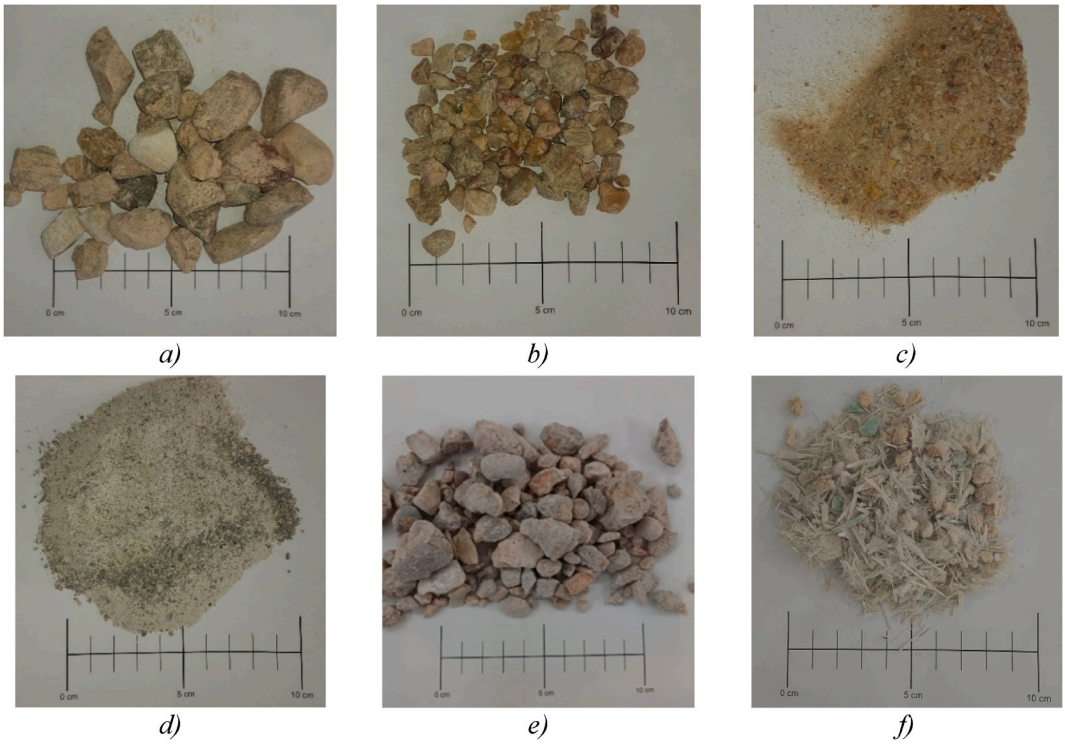

Fig. 2. Materials employed in the experimental campaign: a) siliceous aggregate 12/22 mm; b) siliceous aggregate 4/12 mm; c) siliceous aggregate 0/4 mm; d) limestone aggregate 0/2 mm; e) CRA 4/22 mm; f) RCWTB.

- CRA was incorporated on the basis of volume correction, hence the overall aggregate weight was lower when CRA was employed, due to its reduced density.
- The cement dosage was kept constant at 320 kg/m^3 in all the mixes, whereas the water content was slightly increased when adding the CRA, to maintain the same effective water/cement ratio, due to its higher water demand than the natural aggregate. The total superplasticizer content was kept constant and equal to 1 % of the cement mass.

The mix details are shown in Table 1. Concrete labels are composed of two parts: the former refers to the CRA content, and the latter mentions the RCWTB addition.

2.3. Testing program

Both fresh and hardened properties were investigated in this work. Two curing conditions were performed, *i.e.*, ambient and moist, to detect different strength evolution patterns, due to cement hydration [33].

The slump, fresh density, and air content were measured during casting in fresh concrete samples according to BS EN 12350-2 [32], BS EN 12350-6 [32], and BS EN 12350-7 [32], respectively. Simultaneously, a series of fifteen 100 × 200-mm cylindrical specimens, fifteen 75 × 75 × 275-mm prismatic specimens, and three 100 × 100 × 100-mm cubic specimens were cast *per* concrete mix. After pouring and vibrating the concrete in the molds, the specimens were left in the lab environment (20 ± 2 °C and 50 ± 5 % humidity) for 24 h properly covered with plastic bags to minimize water evaporation.

Three cylinders and three prisms were tested to measure compressive and flexural strength, respectively, after 24 h of curing (concrete age of 1 day). Later on, six cylinders and six prisms were cured in a moist chamber (20 ± 2 °C and 90 ± 5 % humidity), and the remaining specimens in an ambient curing room (20 ± 2 °C and 60 ± 5 % humidity). Three cylinders and three prisms *per* curing environment were tested to establish their compressive and flexural strength at an age of both three and seven days according to European standards BS EN 12390-3 [32] and BS EN 12390-5 [32], respectively. A model was also developed to predict the flexural strength from the compressive strength in this kind of concrete mixes. Hardened density was also measured on the cubic specimens as *per* BS EN 12390-7 [32] after one, three, and seven days of ambient curing.

Plastic shrinkage was measured over the first three days of ambient curing (20 ± 2 °C and 60 ± 5 % humidity) following a procedure developed by the authors [34]. To perform this test, the fresh concrete was poured in a 1-m long gutter. The concrete could freely move at just one end during setting, while the other remained fixed. In this way, the free end was equipped with a digital comparator to measure concrete displacement and, therefore, shrinkage to a precision of ±0.01 mm.

Scanning Electron Microscopy (SEM) and Energy Dispersive X-ray (EDX) analyses of the Interfacial Transition Zones (ITZs) between different components of the RCWTB and the cementitious matrix were also performed in fragments from within the tested specimens. A JEOL JSM-6460LV microscope was used to obtain SEM images at up to 1000x magnification, as well as the EDX spectra. The aim was to further understand the mechanical behavior of the concrete mixtures [35,36].

Finally, all the experimental results were validated through an ANalysis Of VAriance (ANOVA), and a cost analysis was performed to verify the suitability of the concrete mixes produced with both CRA and RCWTB from an economic approach.

3. Results and discussion

3.1. Fresh properties

The results of the fresh tests are displayed in Table 2. A general decrease in workability was recorded after having replaced the conventional coarse aggregate with CRA and after having added the RCWTB. Recycled aggregates usually demonstrate higher interlocking forces between their particles, as they have a more irregular shape and rougher texture, which hinders proper concrete flow [37]. Similarly, the use of fibers within concrete, such as those contained in the RCWTB, interferes with the movement of the other concrete components [38]. Those performances lead to conclude that a higher water/cement ratio is required when CRA is employed in concrete [39,40], even higher if RCWTB is added in the same concrete mix. Indeed, the slump of the 100CRA/6RCWTB mix was only 1 cm.

According to Mehdipour et al. [41], a fiber volume fraction of 2 % leads to a 40 % decrease in workability in concrete containing 12-mm-long glass fibers, while a fiber volume fraction to 3 % results in a reduction of 75 %. In this work, the content by volume of

Table 1
Mix design (in kg/m^3).

	0CRA/0RCWTB	50CRA/0RCWTB	100CRA/0RCWTB	0CRA/6RCWTB	50CRA/6RCWTB	100CRA/6RCWTB
Cement	320	320	320	320	320	320
Water	130	140	150	130	140	150
w/c ratio	0.41	0.44	0.47	0.41	0.44	0.47
Plasticizer 1	1.07	1.07	1.07	1.07	1.07	1.07
Plasticizer 2	2.13	2.13	2.13	2.13	2.13	2.13
Siliceous 12/22 mm	780	390	0	733	367	0
Siliceous 4/12 mm	555	277	0	522	261	0
Siliceous 0/4 mm	385	385	385	362	362	362
Limestone 0/2 mm	280	280	280	263	263	263
CRA 4/22 mm	0	623	1246	0	586	1171
RCWTB	0	0	0	75	75	75

Table 2
Results of fresh tests.

Mix	Slump (cm)	Fresh density (kg/dm^3)	Air content (% vol.)
0CRA/0RCWTB	15	2.46	2.4
50CRA/0RCWTB	17	2.37	2.1
100CRA/0RCWTB	5	2.33	3.2
0CRA/6RCWTB	15	2.39	3.0
50CRA/6RCWTB	13	2.32	3.7
100CRA/6RCWTB	1	2.29	4.1

GFRP-composite fiber in the concrete mixes with RCWTB was around 2.5 %, considering an average fiber density of 2.04 kg/dm^3 [24]. Its addition resulted in workability decreases of 0 %, 25 %, and 80 % when combined with 0 %, 50 %, and 100 % CRA, respectively. Workability worsened as the amounts of CRA increased, although the results were better than those of Mehdipour et al. [41] with up to CRA contents of 50 %, even though recycled fibers were used in this research. Furthermore, the contribution of balsa wood and polymers to worsening workability should not be overlooked.

Fresh density decreased with higher amounts of CRA replacements and when RCWTB was added. The addition of higher amounts of CRA resulted in a linear decrease of fresh density, because of the higher content of adhered mortar within the CRA, which meant that the aggregate had a lower density and a higher porosity than natural aggregate [42]. Furthermore, higher CRA replacements were accompanied by higher water dosages, which further contributed to a more porous microstructure [43]. Analogously, RCWTB additions also decreased fresh density, due to its huge difference in density with the aggregates (about 2.60 kg/m^3 vs.1.63 kg/m^3), a result that Revilla-Cuesta et al. [29] had previously confirmed.

Air content also showed a clear trend, as it increased for higher CRA and RCWTB additions. Thus, the simultaneous addition of 100 % CRA and 6 % RCWTB increased the air content of the concrete by 1.7 % in absolute terms. CRA incorporation in concrete mixtures favors air entrapment within the mix due to its rougher surface and sharp geometry [37]. RCWTB increases air retention due to the presence of fibers [44] and low-density materials, *i.e.*, balsa wood and polymers, with high specific porosity [45,46].

3.2. Hardened density

The results of hardened density are reported in Table 3. Hardened density decreased for higher CRA replacements and RCWTB additions, as did the fresh density. The reasons for such decreases were the same as those explained for fresh density [47]. Moreover, all the concrete mixes underwent a slight weight reduction over time, due to progressive water evaporation during the first days of curing [48], which was slightly favored when RCWTB was incorporated. It should be recalled that the cubic samples for hardened density evaluation were cured in an ambient room (20 $\pm$ 2 °C and 60 $\pm$ 5 % humidity), so water evaporation was favored.

3.3. Plastic shrinkage

The results of the plastic-shrinkage test are depicted in Fig. 3. Most of the plastic shrinkage took place during the first 10 h of the curing process, after which shrinkage gradually slowed down. All the concrete mixes underwent shrinkage, which was lower than −0.7 mm/m over 72 h of ambient curing in absolute value, except for the 100CRA/0RCWTB mix, which showed a significantly higher shrinkage rate, *i.e.*, −1.07 mm/m, 3 days after casting.

CRA additions usually affect shrinkage, as that waste demonstrates higher flexibility and water absorption than natural aggregates [49]. An amount of 50 % CRA insignificantly affected plastic shrinkage, while it was widely increased when 100 % CRA was added. Thus, after 72 h of ambient curing, the 100CRA/0RCWTB mix showed 70 % higher plastic shrinkage than that of the 0CRA/0RCWTB reference mix, whereas that increase for the 50CRA/0RCWTB mix was just 3 %.

The addition of RCWTB significantly helped reduce plastic shrinkage. The GFRP-composite fibers contained in the RCWTB clearly developed the bridging effect traditionally found in fiber-reinforced concrete produced with commercial fibers [50]. Therefore, RCWTB additions resulted in a well-bonded matrix that hindered high dilatations and contractions, because the GFRP-composite fibers acted as rigid elements within the cementitious matrix [51]. This decrease was more notable when the CRA content was high, which may be caused by the frictional behavior of the GFRP-composite fibers with rough CRA particles [18]. Thus, for example, shrinkage contraction after 3 days from casting was reduced by 47 % when RCWTB was added to concrete containing 100 % CRA, whereas a reduction of only 21 % was recorded when RCWTB was employed in conventional concrete with exclusively natural aggregates. As an overall result of these two phenomena, a negligible difference in plastic shrinkage was found when varying the CRA replacement ratio in concrete incorporating 6 % RCWTB.

Table 3
Hardened density (kg/dm^3).

Mix	1 day	3 days	7 days
0CRA/0RCWTB	2.45	2.43	2.43
50CRA/0RCWTB	2.37	2.36	2.36
100CRA/0RCWTB	2.34	2.33	2.32
0CRA/6RCWTB	2.36	2.36	2.35
50CRA/6RCWTB	2.32	2.31	2.31
100CRA/6RCWTB	2.3	2.29	2.28

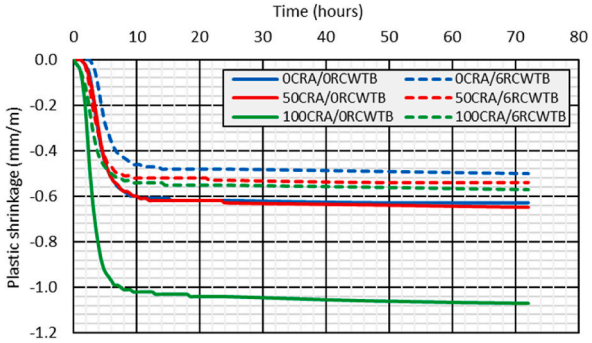

Fig. 3. Plastic shrinkage: Evolution over three days.

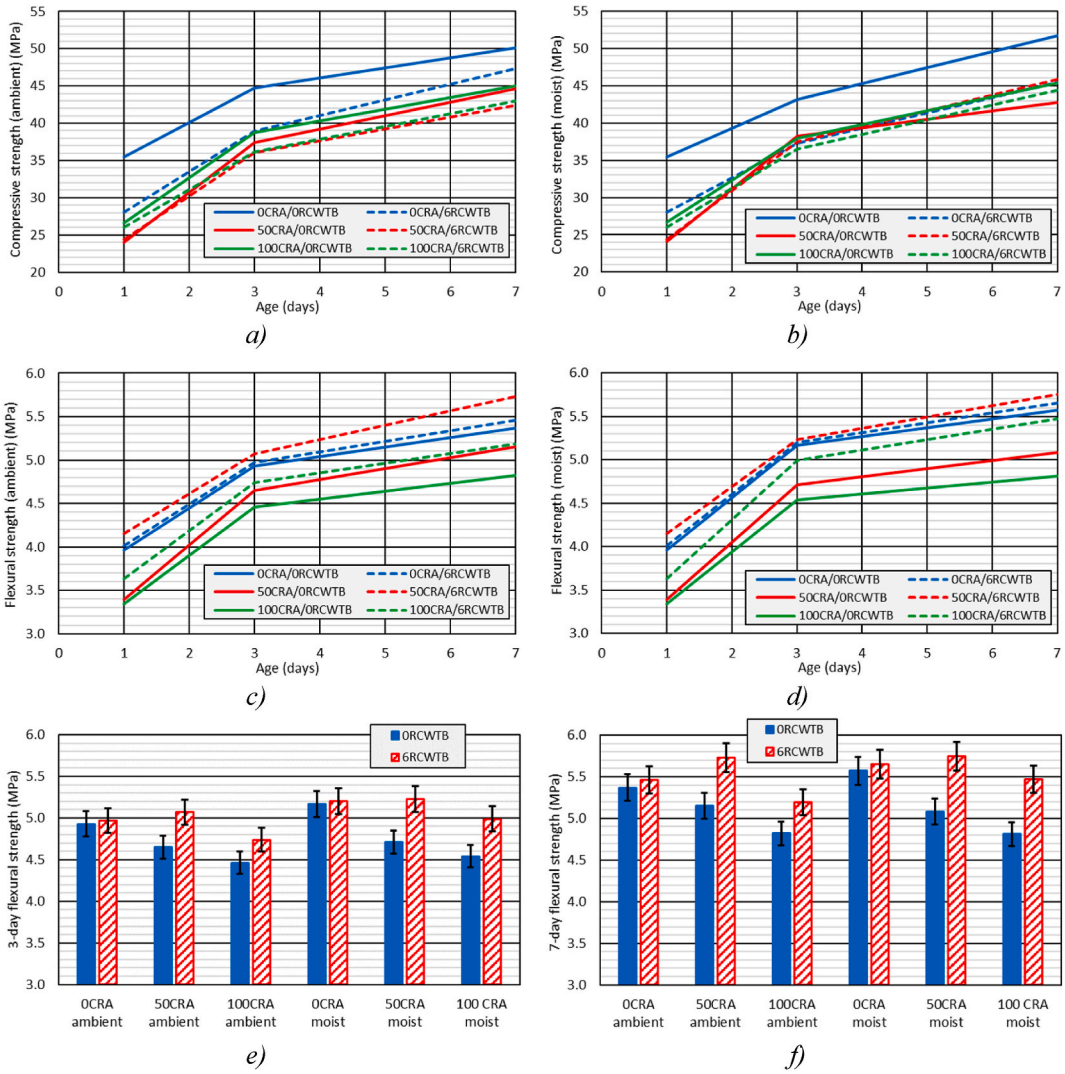

Fig. 4. Strength test results: a) compressive strength evolution under ambient curing; b) compressive strength evolution under moist curing; c) flexural strength evolution under ambient curing; d) flexural strength evolution under moist curing; e) effect of RCWTB in 3-day flexural strength; f) effect of RCWTB in 7-day flexural strength.

3.4. Mechanical properties

3.4.1. Compressive strength

The results of compressive strength are displayed in Fig. 4a for ambient curing and in Fig. 4b for moist curing. As a first outcome, all the concrete mixes exceeded a 7-day compressive strength of 40 MPa for both curing conditions, demonstrating suitable strengths for structural applications according to the European standard BS EN 1992-1-1 (Eurocode 2) [32].

As foreseen, the 0CRA/0RCWTB conventional mix showed the highest compressive strength, because the inclusion of both RCWTB and CRA tended to decrease that strength, as clearly reported in the literature [29,52]:

- CRA is generally responsible for a strength decrease when incorporated in concrete, due to the old mortar layer attached to its surface, which is soft and highly porous. Furthermore, two different ITZs can be identified in concrete produced with CRA: the former between the natural aggregate and the old mortar, and the latter between CRA and the new cementitious matrix [8]. Both aspects worsen ITZs, resulting in lower strength, as ITZs are considered the weakest part of concrete where cracking initiates and from within which it is propagated [35,36].
- RCWTB usually causes a similar phenomenon, as the presence of balsa wood and polymeric particles weakens some ITZs, because of their poor adhesion within the cementitious matrix [53]. Furthermore, the bridging effect of the GFRP-composite fibers is more effective at improving flexural strength and deformational behavior rather than compressive strength [54]. Therefore, the use of this waste mostly led to small reductions in compressive strength in this experimental campaign. For example, the incorporation of 6 % RCWTB lowered the compressive strength of the concrete with 0 % CRA by 6 % after 7 days of ambient curing. In contrast, a reduction of only 5 % was recorded for both 50 % CRA and 100 % CRA replacement ratios, and the RCWTB once again showed suitable interaction with CRA. Similar trends were obtained under moist curing, except for concrete containing 50 % CRA, whose compressive strength increased by 7 % when adding 6 % RCWTB, due to the optimum interaction between both wastes. He et al. [55] had previously demonstrated the beneficial effect of hybrid steel and polypropylene fibers on the mechanical properties of RAC. A noteworthy aspect is that similar behavior was also obtained in this case by adding RCWTB, which is a waste material.

Another factor analyzed here is the strength evolution over time. Moist curing is widely considered essential to achieve higher concrete strengths [56], as it favors cement hydration despite any different compositions [57]. An observation that was experimentally confirmed in this research, with just a few exceptions. Furthermore, it is interesting to note that, were the 0CRA/0RCWTB mix not considered, the strength values of the mixtures after ambient curing could have been more divergent, whereas similar strengths were observed for moist curing, as well as more beneficial effects of RCWTB added to concrete mixes containing CRA.

3.4.2. Flexural strength

The results of flexural strength are shown in Fig. 4c and d for ambient and moist curing, respectively. After 7 days of curing in both environmental conditions, all the concrete mixes reached a flexural strength of at least 4.5 MPa.

Focusing exclusively on the concrete mixes with no RCWTB, lower strengths were recorded as CRA content increased. The 0CRA/0RCWTB mix had the highest strength at all ages for both curing conditions. On the other hand, the 50CRA/0RCWTB and 100CRA/0RCWTB mixes demonstrated almost the same 1-day flexural strength, but the strength of the mix with 50 % CRA rose over the curing time, thus its 7-day flexural strength was 7 % higher. The lower flexural strength recorded for higher CRA replacements was due to the same reasons as for compressive strength, *i.e.*, more porous and softer ITZs after aggregate additions, and higher water dosages employed in the mixtures that they contained [58].

In contrast to compressive strength, the inclusion of RCWTB was highly beneficial in terms of flexural strength. No enhancements in this strength were generally recorded when RCWTB was added to conventional concrete [29], but a notable improvement in flexural strength could be perceived when RCWTB was combined with 50 % CRA and 100 % CRA. That behavior is clearly visible in Fig. 4e and f, at 3 and 7 days of curing, respectively. After 7 days of ambient curing, additions of RCWTB led to higher flexural strengths of 2 %, 11 %, and 8 % moving from 0 % CRA to 100 % CRA. Similarly, the strength increases were equal to 1 %, 13 %, and 14 % for moist curing. The combination of 50 % CRA and RCWTB was particularly beneficial, as the 50CRA/6RCWTB mix surpassed the flexural strength of both mixtures with 0 % CRA for all curing times and conditions.

The results demonstrated that RCWTB can effectively compensate the detrimental effects that CRA can have on the development of flexural strength, which was slightly improved after conducting moist curing. GFRP-composite fibers contained in RCWTB were no doubt responsible for that favorable effect on strength performance, thanks to their bridging effect within the cementitious matrix [54]. Furthermore, the optimal interaction between both residues should also be highlighted, as the improvement in flexural strength was higher when RCWTB was combined with CRA, a fact also found in previous works in the literature for other fiber types [18,20]. The weak bond between the cementitious matrix and the CRA means that the fibers have a more significant impact on the tensile properties of concrete than when using natural aggregates, as they effectively limit the development of microcracks in the ITZs [19]. It can even be suggested that the bridging effect of the GFRP-composite fibers could be favored by their friction with CRA particles, which had a rough surface [59].

Xu et al. [60] found a strength increase equal to 4.34 %, 13.30 %, and 37.85 % for fiber volume ratios of 0.5 %, 1.5 %, and 2.5 %, respectively, by employing macro-fibers from decommissioned wind-turbined blades. Rodin et al. [61] obtained the highest strength increase when employing recycled GFRP-composite fibers from end-of-life wind-turbine blades at a percentage of 5 % by volume. In this work, an evident improvement was also recorded with 6 % of RCWTB by volume, although it should be noted that RCWTB also includes particles of balsa wood and polymers, which partially jeopardize the beneficial effect of GFRP-composite fibers, but that facilitate recovery and recycling of wind-turbine blades. Furthermore, this is the first time in the literature that the validity of this

waste to improve the performance of concrete containing CRA has been addressed and demonstrated.

3.4.3. Prediction of flexural strength

The prediction of flexural strength from compressive strength is of undoubted utility for many design applications. However, the relationship between both strengths when alternative raw materials are employed for concrete production is not the same as for conventional concrete. In this section, the relationship between compressive and flexural strengths is analyzed to establish a model with which to predict the early-age flexural strength.

The features of the models specified in the standards (BS EN 1992-1-1, Eurocode 2 [32]) were followed for the development of this predictive model. Therefore, apart from considering compressive strength as an independent variable, a time dependence logarithmic factor was introduced to improve accuracy. The relationship between all these variables was first analyzed in terms of a simple regression, which showed the existence of autocorrelation between the residuals, leading to the invalidity of the models developed in this procedure. This problem was solved through the Cochrane-Orcutt method, which estimated the error term of the relationship through a linear model [62]. The result was the model detailed in Eq. (1), in which *FS* is the flexural strength of the concrete mix, in MPa, which is to be estimated; *CS* is the compressive strength of the concrete mix, also in MPa; and *t* is the concrete age, in days.

$$FS = 3.138 + 0.026 \times CS + 0.550 \times \ln(t) \quad (1)$$

This model yielded an R^2 coefficient of 88.26 %, a Mean Absolute Error (MAE) of 0.251, and a value of the Durbin-Watson statistic of 1.809. The coefficient R^2 provides information on the goodness of fit of a model. In this case, a high R^2 reflected a good fit with the experimental data. The MAE indicates the average absolute error between predicted and experimental values, so a MAE close to 0 demonstrates good alignment with the experimental results. The Durbin-Watson statistic is useful to detect autocorrelation in the residuals from a regression analysis. In this particular case, the statistic had a higher value than 1.566, indicating that there was no autocorrelation. Those three parameters confirmed the estimation quality of the model and the randomness of the residual distribution. Adequate predictive accuracy was also confirmed, in so far as the maximum deviation between the experimental and predicted flexural strengths of the mixes was around 10 % in absolute terms, as shown in Fig. 5.

3.5. Statistical analysis: ANOVA

To statistically validate the experimental results, an ANOVA was performed for all the properties with a confidence level of 95 %, considering all the experimental values and not only the average values reported in previous sections [31]. The factors analyzed were the CRA content (factor A), the RCWTB content (factor B), the testing age (factor C), and the type of curing (factor D). Table 4 lists the *p*-values for each factor, while Table 5 shows the *p*-values for the second-order interactions. The effect of the factors and interactions was significant when their *p*-values were less than 0.05.

Regarding the effect of the factors, all the properties of concrete were significantly affected by the content of both wastes. Only the testing age in relation to hardened density and the type of curing regarding compressive strength were not significant. In terms of second-order interactions, only the interaction between the CRA and RCWTB contents was in general significant. Therefore, the behavior of concrete containing CRA was strongly modified by RCWTB addition, which allowed notably improving concrete performance in different terms, such as plastic shrinkage and flexural strength. This statistical analysis therefore validates the discussions previously conducted in the paper.

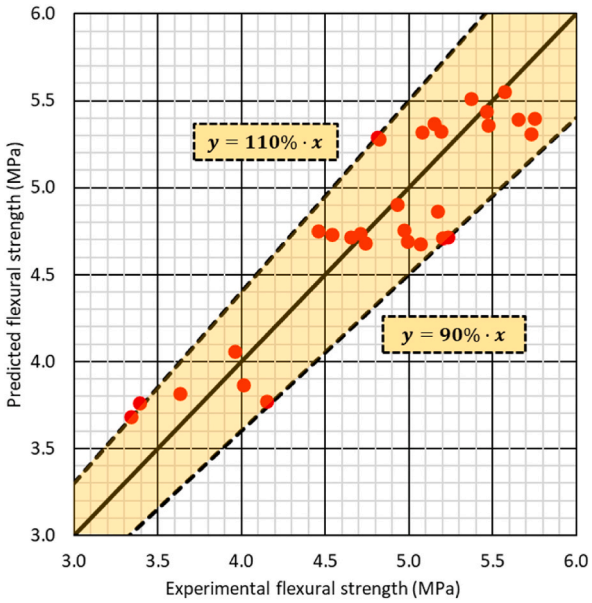

Fig. 5. Comparison between experimental and predicted flexural strengths.

Table 4
p-values for the factors according to ANOVA.

Property	CRA content (factor A)	RCWTB content (factor B)	Age (factor C)	Curing (factor D)
Slump	0.0000	0.0000	–	–
Fresh density	0.0001	0.0006	–	–
Air content	0.0002	0.0000		
72-h plastic shrinkage	0.0000	0.0000	–	–
Hardened density	0.0000	0.0000	0.0520	–
Compressive strength	0.0000	0.0000	0.0000	0.7571
Flexural strength	0.0000	0.0000	0.0000	0.0101

Table 5
p-values for the second-order interactions according to ANOVA.

Property	A:B	A:C	A:D	B:C	B:D	C:D
Slump	0.0106	–	–	–	–	–
Fresh density	0.3732	–	–	–	–	–
Air content	0.0064	–	–	–	–	–
72-h plastic shrinkage	0.0001	–	–	–	–	–
Hardened density	0.0075	0.9526	–	0.8478	–	–
Compressive strength	0.0000	0.0110	0.3226	0.4051	0.4512	0.6259
Flexural strength	0.0000	0.5619	0.3736	0.3501	0.3007	0.1260

The letters refer to each factor analyzed according to Table 4.

3.6. Microstructural analysis

Microstructural tests were performed to further understand the mechanisms that led to the early-age behavior exhibited by the concrete mixes with CRA and RCWTB. Fig. 6 shows the Scanning Electron Microscopy (SEM) images of the ITZs for both a GFRP-composite fiber and a polymeric particle. Furthermore, Figs. 7 and 8 depict the EDX spectra for the same GFRP-composite fiber and polymeric particle, respectively.

Regarding the GFRP-composite fibers, their optimal adhesion to the cementitious matrix could be detected (Fig. 6a and b), as their ends were perfectly embedded in the cementitious matrix after failure. A behavior that the irregular surface of the GFRP epoxy resin matrix might favor [24]. It was even noted that tiny cementitious matrix fragments remained adhered to the surface of the part of the fibers that slipped and failed during flexural strength testing (Fig. 6c). These tiny fragments were also detected through EDX spectra (Fig. 7), since the spectrum performed on the GFRP-composite fiber showed high proportions of calcium and silica despite its composition based on fiberglass and epoxy resin. Thus, its composition was very similar to that of the surrounding cementitious matrix, in which the GFRP-composite fiber was embedded. All those aspects successfully improved both plastic shrinkage and flexural strength when adding RCWTB to concrete containing CRA.

The GFRP-composite fibers worked less effectively in terms of compressive strength, so the weak particles, such as polymeric ones, had greater influence than any others on strength [53]. Furthermore, those particles showed ITZs of low adhesion, as can be seen in Fig. 6d and e. A clear separation between the cementitious matrix and the particles could be observed in all cases, which favored the sliding effect between both when applying load. It could in fact be seen in those images that the polymeric particles never broke during loading, which might otherwise have happened, if there had been high adhesion between them and the cementitious matrix [35]. Finally, the EDX spectra (Fig. 8) clearly showed the absence of cementitious matrix adhered to the surface of the polymeric particle, since the components that predominated in the spectrum conducted on it were carbon and oxygen. Thus, it is clear that the polymer particles detached from the cementitious matrix when the concrete was loaded, which resulted in small decreases in compressive strength.

3.7. Cost based on raw materials

The widespread use of the concrete mixes analyzed in this research requires that they are economically competitive [2]. Thus, to conclude the study, an analysis of the cost of the concrete mixes exclusively based on the cost of their raw materials was conducted. The cost of the transportation of the concrete or the energy consumed during its mixing, among other aspects, were not considered. This analysis intended to perform a first approach to the effect of the addition of CRA and RCWTB in concrete only in terms of the cost of raw-material acquisition.

Therefore, in line with the above, the determination of the cost of each concrete mix was based on multiplying the cost of each raw material and its amount in a cubic meter of concrete (Table 1) [3]. The cost of all the raw materials (Table 6) was obtained from official price databases of Spain [63], where the study was conducted, except for RCWTB, whose price was obtained from estimates made by the waste producers. The results obtained for the different concrete mixes (Fig. 9) showed that the cost of the concrete decreased by around 4.2 % when 50 % CRA was added, while the decrease due to the addition of 6 % RCWTB was only around 0.75 %. Both wastes made the concrete cheaper, as usually reported in the literature [2,3], although today's more industrialized CRA production and its use in higher amounts in concrete resulted in a further decrease in cost due to it.

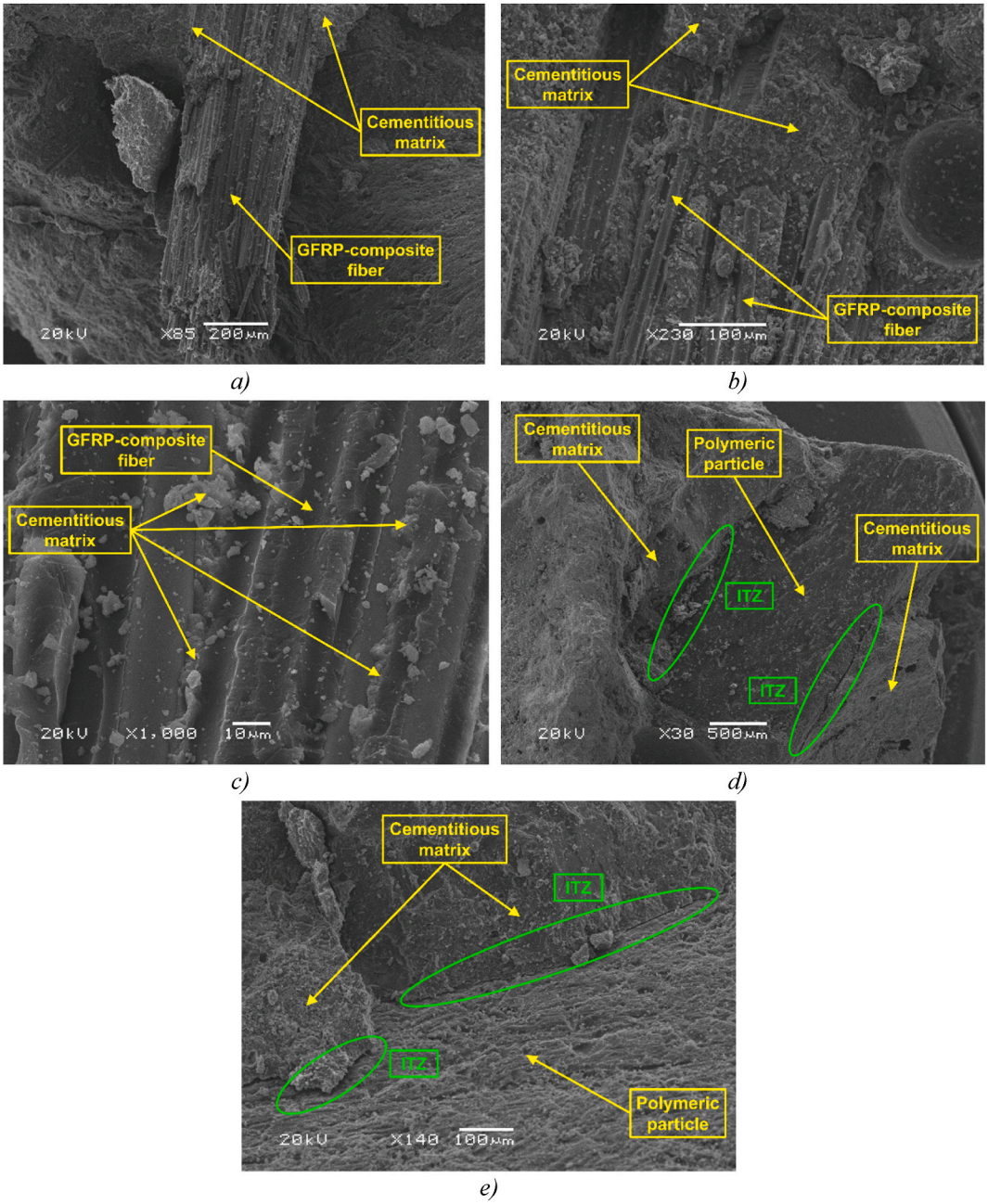

Fig. 6. SEM images of ITZs between RCWTB components and the cementitious matrix: a-c) GFRP-composite fiber; d-e) polymeric particle.

4. Concluding remarks

In this research, a sustainable method has been proposed to improve the properties of concrete containing Coarse Recycled Aggregate (CRA). Raw-Crushed Wind-Turbine Blade (RCWTB) containing fibers from the crushing of Glass Fiber-Reinforced Polymer (GFRP) composite, balsa wood and polymers was employed as an addition in concrete to improve some critical properties of the concrete incorporating that sustainable aggregate. The RCWTB was incorporated in contents equal to 0 % and 6 % by volume, whereas the content of CRA ranged from 0 % to 100 %. Having completed this study, the following conclusions can be drawn:

- Workability and fresh density decreased when CRA and RCWTB were included in the concrete mix, while the air content increased. The irregular shape and rougher texture of CRA hindered concrete flow, in the same way as the GFRP-composite fibers present in the RCWTB. Both aspects led to a reduction in concrete workability. The lower density and the higher porosity of CRA and RCWTB led to the described performance in terms of fresh density and air content.

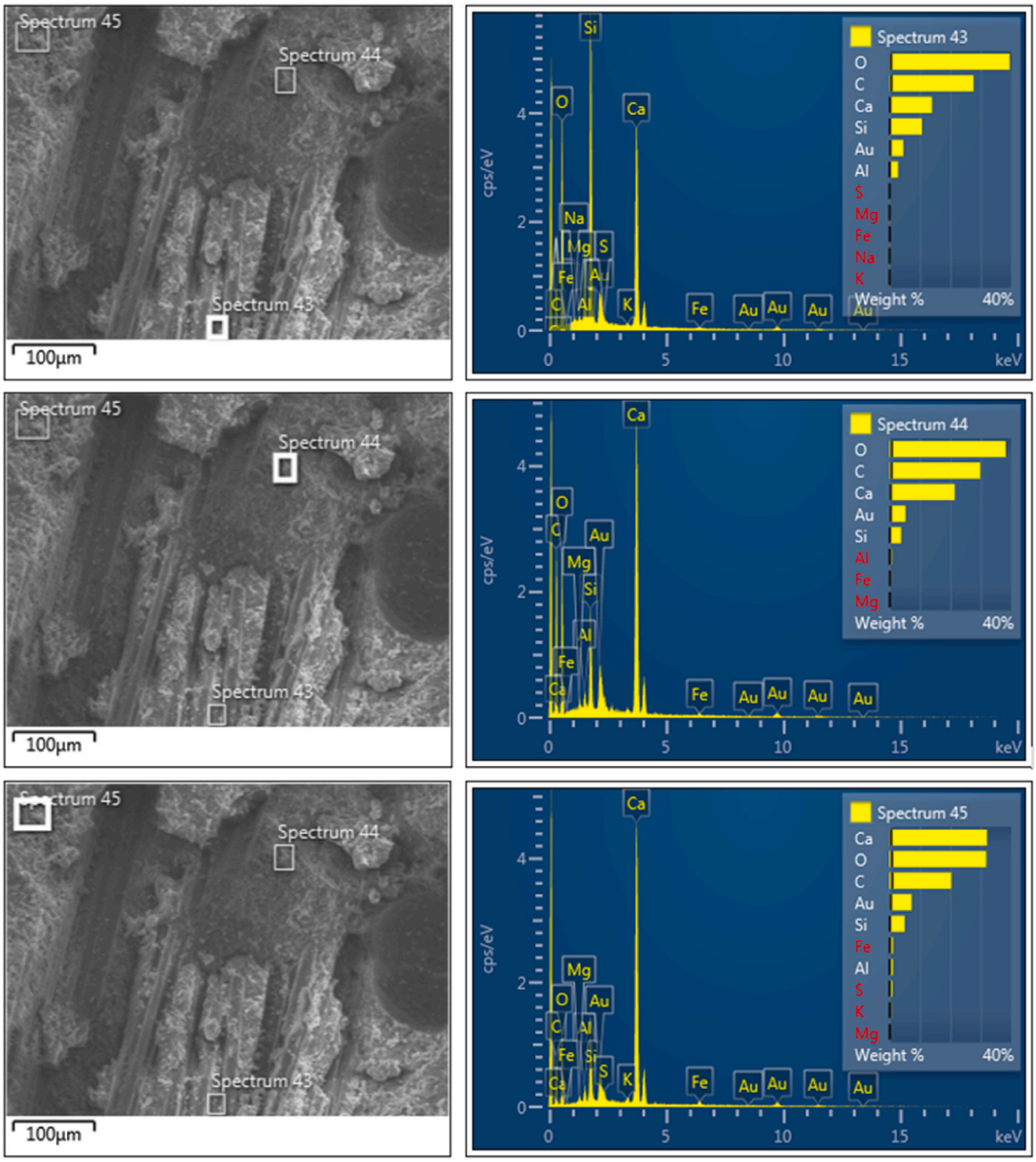

Fig. 7. EDX spectra of a GFRP-composite fiber.

- The inclusion of RCWTB in the concrete was highly effective at decreasing plastic shrinkage, particularly when the content of CRA was high. The GFRP-composite fibers present in the RCWTB successfully acted as rigid elements within the concrete matrix, limiting this contraction. Thus, the plastic shrinkage over three days of ambient curing was reduced by 47 % when RCWTB was added to concrete containing 100 % CRA.
- The simultaneous use of CRA and RCWTB resulted in a concrete that surpassed 40 MPa of compressive strength after 7 days of curing, demonstrating their suitability for structural applications. However, the inclusion of RCWTB slightly lowered the compressive strength of the mixtures. This was because the GFRP-composite fibers of RCWTB did not work effectively when compressive stresses were applied, and the polymeric particles showed a poor adhesion to the cementitious matrix.
- All concretes reached at least 4.5 MPa of flexural strength after 7 days of curing. The incorporation of RCWTB effectively compensated the detrimental effects of using CRA in concrete in terms of flexural strength. An effect that may be explained by the optimal adhesion of the GFRP-composite fibers within the cementitious matrix, which was verified through scanning electron microscopy. The effect was more beneficial under moist curing conditions. The mixture including 6 % RCWTB, and 50 % CRA even exhibited a higher flexural strength than the concrete manufactured without CRA, probably due to the friction of some GFRP-composite fibers with CRA particles.

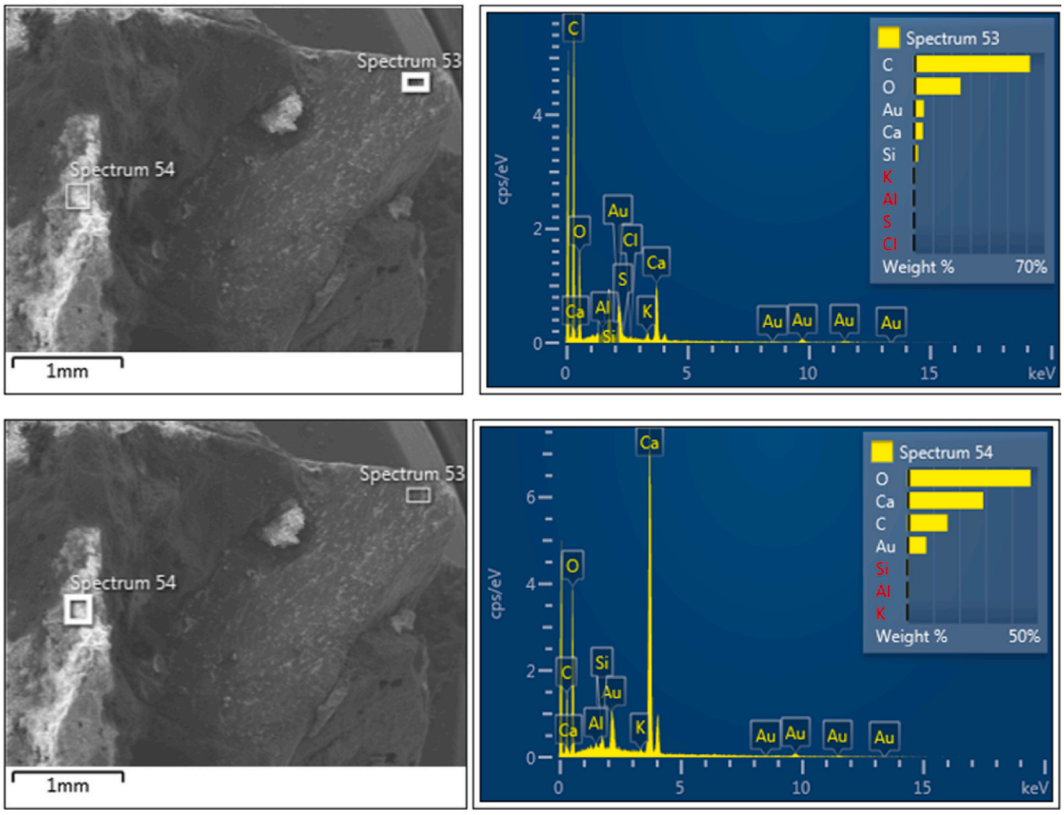

Fig. 8. EDX spectra of a polymeric particle.

Table 6
Cost of the raw materials of concrete.

Raw material	Cost (€/kg)
Cement	0.0962
Water	0.0006
Plasticizer 1	1.3700
Plasticizer 2	1.3700
Siliceous 12/22 mm	0.0068
Siliceous 4/12 mm	0.0067
Siliceous 0/4 mm	0.0085
Limestone 0/2 mm	0.0058
CRA 4/22 mm	0.0038
RCWTB	0.0052

- A time-dependent Cochrane-Orcutt model was proposed and validated to predict the early-age flexural strength of concrete with CRA and RCWTB through the compressive strength. Therefore, this type of regression model is suitable for relating these two properties in concrete made simultaneously with CRA and RCWTB.

In general, this work has revealed that the use of 6 % RCWTB can significantly reduce plastic-shrinkage rates and improve the flexural strength of concrete containing CRA mainly under a moist curing, whilst preserving its compressive strength. Moreover, RCWTB even slightly reduces the cost of concrete. However, the composition of RCWTB can vary depending on the origin of the wind-turbine blades and even their geographic location. Therefore, the analysis of concrete containing RCWTB from a wide variety of wind-turbine blades would allow a wider generalization of the conclusions reached in this study. Future research should be conducted in this regard.

CRediT authorship contribution statement

Daniel Trento: Writing – review & editing, Writing – original draft, Software, Investigation, Formal analysis. **Flora Faleschini:** Validation, Supervision, Methodology, Investigation, Data curation. **Víctor Revilla-Cuesta:** Writing – review & editing, Visualization, Methodology, Investigation, Formal analysis, Conceptualization. **Vanesa Ortega-López:** Writing – review & editing, Supervision,

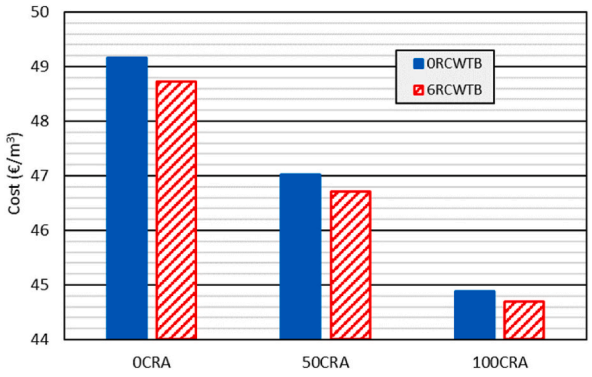

Fig. 9. Cost of the concrete mixes.

Resources, Project administration, Funding acquisition, Conceptualization.

Declaration of competing interest

The authors declare that they have no known competing financial interests or personal relationships that could have appeared to influence the work reported in this paper.

Data availability

Data will be made available on request.

Acknowledgements

This research work was supported by MICINN, AEI, EU, ERDF and NextGenerationEU/PRTR [grant numbers PID2023-146642OB-I00; 10.13039/501100011033; TED2021-129715B–I00]; the Junta de Castilla y León (Regional Government) and ERDF [grant number UIC-231; BU033P23]; the University of Burgos [grant number SUCONS, Y135.GI]; and, finally, the University of Padova. Finally, the authors wish to pass on their sincere thanks to Manuel Hernando-Revenga, Nerea Hurtado-Alonso, Javier Manso-Morato and Marcos Villalaín-Soto for their useful assistance during the lab work.

References

[1] C.R. Gagg, Cement and concrete as an engineering material: an historic appraisal and case study analysis, Eng. Fail. Anal. 40 (2014) 114–140, https://doi.org/10.1016/j.engfailanal.2014.02.004.
[2] S. Saha, D. Sau, T. Hazra, Economic viability analysis of recycling waste plastic as aggregates in green sustainable concrete, Waste Manage. (Tucson, Ariz.) 169 (2023) 289–300, https://doi.org/10.1016/j.wasman.2023.07.023.
[3] F.K. Alqahtani, I.S. Abotaleb, M. El Menshawy, Life cycle cost analysis of lightweight green concrete utilizing recycled plastic aggregates, J. Build. Eng. 40 (2021) 102670, https://doi.org/10.1016/j.jobe.2021.102670.
[4] S. Tejas, D. Pasla, Assessment of mechanical and durability properties of composite cement-based recycled aggregate concrete, Construct. Build. Mater. 387 (2023) 131620, https://doi.org/10.1016/j.conbuildmat.2023.131620.
[5] A. Akhtar, A.K. Sarmah, Construction and demolition waste generation and properties of recycled aggregate concrete: a global perspective, J. Clean. Prod. 186 (2018) 262–281, https://doi.org/10.1016/j.jclepro.2018.03.085.
[6] K. Kabirifar, M. Mojtahedi, C. Wang, V.W.Y. Tam, Construction and demolition waste management contributing factors coupled with reduce, reuse, and recycle strategies for effective waste management: a review, J. Clean. Prod. 263 (2020) 121265, https://doi.org/10.1016/j.jclepro.2020.121265.
[7] M.C. Collivignarelli, G. Cillari, P. Ricciardi, M.C. Miino, V. Torretta, E.C. Rada, A. Abbà, The production of sustainable concrete with the use of alternative aggregates: a review, Sustainability 12 (19) (2020) 7903, https://doi.org/10.3390/SU12197903.
[8] B. Wang, L. Yan, Q. Fu, B. Kasal, A comprehensive review on recycled aggregate and recycled aggregate concrete, Resour. Conserv. Recycl. 171 (2021) 105565, https://doi.org/10.1016/j.resconrec.2021.105565.
[9] J.A. Forero, J. de Brito, L. Evangelista, C. Pereira, Improvement of the quality of recycled concrete aggregate subjected to chemical treatments: a review, Materials 15 (8) (2022) 2740, https://doi.org/10.3390/ma15082740.
[10] V.W.Y. Tam, M. Soomro, A.C.J. Evangelista, Quality improvement of recycled concrete aggregate by removal of residual mortar: a comprehensive review of approaches adopted, Construct. Build. Mater. 288 (2021) 123066, https://doi.org/10.1016/j.conbuildmat.2021.123066.
[11] L. Wang, J. Wang, X. Qian, P. Chen, Y. Xu, J. Guo, An environmentally friendly method to improve the quality of recycled concrete aggregates, Construct. Build. Mater. 144 (2017) 432–441, https://doi.org/10.1016/j.conbuildmat.2017.03.191.
[12] S. Jamil, J. Shi, M. Idrees, Effect of various parameters on carbonation treatment of recycled concrete aggregate using the design of experiment method, Construct. Build. Mater. 382 (2023) 131339, https://doi.org/10.1016/j.conbuildmat.2023.131339.
[13] N. Kisku, H. Joshi, M. Ansari, S.K. Panda, S. Nayak, S.C. Dutta, A critical review and assessment for usage of recycled aggregate as sustainable construction material, Construct. Build. Mater. 131 (2017) 721–740, https://doi.org/10.1016/j.conbuildmat.2016.11.029.
[14] C. Shi, Y. Li, J. Zhang, W. Li, L. Chong, Z. Xie, Performance enhancement of recycled concrete aggregate - a review, J. Clean. Prod. 112 (2016) 466–472, https://doi.org/10.1016/j.jclepro.2015.08.057.
[15] F. Aslani, J. Kelin, Assessment and development of high-performance fibre-reinforced lightweight self-compacting concrete including recycled crumb rubber aggregates exposed to elevated temperatures, J. Clean. Prod. 200 (2018) 1009–1025, https://doi.org/10.1016/j.jclepro.2018.07.323.
[16] K.J.N.S. Nitesh, S.V. Rao, P.R. Kumar, An experimental investigation on torsional behaviour of recycled aggregate based steel fiber reinforced self compacting concrete, J. Build. Eng. 22 (2019) 242–251, https://doi.org/10.1016/j.jobe.2018.12.011.

[17] R. Chan, X. Liu, I. Galobardes, Parametric study of functionally graded concretes incorporating steel fibres and recycled aggregates, Construct. Build. Mater. 242 (2020) 118186, https://doi.org/10.1016/j.conbuildmat.2020.118186.
[18] W. Ahmed, C.W. Lim, Production of sustainable and structural fiber reinforced recycled aggregate concrete with improved fracture properties: a review, J. Clean. Prod. 279 (2021) 123832, https://doi.org/10.1016/j.jclepro.2020.123832.
[19] D. Gao, L. Zhang, J. Zhao, P. You, Durability of steel fibre-reinforced recycled coarse aggregate concrete, Construct. Build. Mater. 232 (2020) 117119, https://doi.org/10.1016/j.conbuildmat.2019.117119.
[20] C.R. Meesala, Influence of different types of fiber on the properties of recycled aggregate concrete, Struct. Concr. 20 (5) (2019) 1656–1669, https://doi.org/10.1002/suco.201900052.
[21] S.A. Hadigheh, F. Ke, S. Kashi, 3D acid diffusion model for FRP-strengthened reinforced concrete structures: long-term durability prediction, Construct. Build. Mater. 261 (2020) 120548, https://doi.org/10.1016/j.conbuildmat.2020.120548.
[22] A. Yazdanbakhsh, L.C. Bank, Y. Tian, Mechanical processing of GFRP waste into large-sized pieces for use in concrete, Recycling 3 (1) (2018) 8, https://doi.org/10.3390/recycling3010008.
[23] S. Karuppannan Gopalraj, T. Kärki, A review on the recycling of waste carbon fibre/glass fibre-reinforced composites: fibre recovery, properties and life-cycle analysis, SN Appl. Sci. 2 (2020) 433, https://doi.org/10.1007/s42452-020-2195-4.
[24] V. Revilla-Cuesta, M. Skaf, V. Ortega-López, J.M. Manso, Raw-crushed wind-turbine blade: waste characterization and suitability for use in concrete production, Resour. Conserv. Recycl. 198 (2023) 107160, https://doi.org/10.1016/j.resconrec.2023.107160.
[25] L. Ziegler, E. Gonzalez, T. Rubert, U. Smolka, J.J. Melero, Lifetime extension of onshore wind turbines: a review covering Germany, Spain, Denmark, and the UK, Renew. Sustain. Energy Rev. 82 (2018) 1261–1271, https://doi.org/10.1016/j.rser.2017.09.100.
[26] A. Cooperman, A. Eberle, E. Lantz, Wind turbine blade material in the United States: quantities, costs, and end-of-life options, Resour. Conserv. Recycl. 168 (2021) 105439, https://doi.org/10.1016/j.resconrec.2021.105439.
[27] Electric Power Research Institute (EPRI), End-of-life Disposal and Recycling Options for Wind Turbine Blades, California, Palo Alto, 2018.
[28] Wind Europe, Wind delivers the energy society wants, (n.d.). https://windeurope.org/about-wind/wind-energy-today/(accessed March 12, 2024).
[29] V. Revilla-Cuesta, J. Manso-Morato, N. Hurtado-Alonso, M. Skaf, V. Ortega-López, Mechanical and environmental advantages of the revaluation of raw-crushed wind-turbine blades as a concrete component, J. Build. Eng. 82 (2024) 108383, https://doi.org/10.1016/j.jobe.2023.108383.
[30] J. Joustra, B. Flipsen, R. Balkenende, Structural reuse of wind turbine blades through segmentation, Comp, Part C: Open Access 5 (2021) 100137, https://doi.org/10.1016/j.jcomc.2021.100137.
[31] V. Revilla-Cuesta, F. Faleschini, C. Pellegrino, M. Skaf, V. Ortega-López, Water transport and porosity trends of concrete containing integral additions of raw-crushed wind-turbine blade, Dev. Built Environ. 17 (2024) 100374, https://doi.org/10.1016/j.dibe.2024.100374.
[32] European Committee for Standardization, BS EN Euronorm, Rue de Stassart 36, 2023. Belgium 1050, Brussels.
[33] C.D. Atiş, F. Özcan, A. Kiliç, O. Karahan, C. Bilim, M.H. Severcan, Influence of dry and wet curing conditions on compressive strength of silica fume concrete, Build. Environ. 40 (2005) 1678–1683, https://doi.org/10.1016/j.buildenv.2004.12.005.
[34] V. Ortega-López, V. Revilla-Cuesta, A. Santamaría, A. Orbe, M. Skaf, Microstructure and dimensional stability of slag-based high-workability concrete with steelmaking slag aggregate and fibers, J. Mater. Civ. Eng. 34 (9) (2022) 04022224, https://doi.org/10.1061/(asce)mt.1943-5533.0004372.
[35] K.L. Scrivener, A.K. Crumbie, P. Laugesen, The interfacial transition zone (ITZ) between cement paste and aggregate in concrete, Interface Sci. 12 (2004) 411–421, https://doi.org/10.1023/B:INTS.0000042339.92990.4c.
[36] B.J. Zhan, D.X. Xuan, C.S. Poon, K.L. Scrivener, Characterization of interfacial transition zone in concrete prepared with carbonated modeled recycled concrete aggregates, Cement Concr. Res. 136 (2020) 106175, https://doi.org/10.1016/j.cemconres.2020.106175.
[37] J. Lavado, J. Bogas, J. de Brito, A. Hawreen, Fresh properties of recycled aggregate concrete, Construct. Build. Mater. 233 (2020) 117322, https://doi.org/10.1016/j.conbuildmat.2019.117322.
[38] D. Ravichandran, P.R. Prem, S.K. Kaliyavaradhan, P.S. Ambily, Influence of fibers on fresh and hardened properties of Ultra High Performance Concrete (UHPC)—a review, J. Build. Eng. 57 (2022) 104922, https://doi.org/10.1016/j.jobe.2022.104922.
[39] J. Montero, S. Laserna, Influence of effective mixing water in recycled concrete, Construct. Build. Mater. 132 (2017) 343–352, https://doi.org/10.1016/j.conbuildmat.2016.12.006.
[40] R.S. Ravindrarajah, Y.H. Loo, C.T. Tam, Recycled concrete as fine and coarse aggregates in concrete, Mag. Concr. Res. 39 (1987) 214–220, https://doi.org/10.1680/macr.1987.39.141.214.
[41] I. Mehdipour, N.A. Libre, M. Shekarchi, M. Khanjani, Effect of workability characteristics on the hardened performance of FRSCCMs, Construct. Build. Mater. 40 (2013) 611–621, https://doi.org/10.1016/j.conbuildmat.2012.11.051.
[42] R.V. Silva, J. de Brito, R.K. Dhir, Fresh-state performance of recycled aggregate concrete: a review, Construct. Build. Mater. 178 (2018) 19–31, https://doi.org/10.1016/j.conbuildmat.2018.05.149.
[43] Z. Lafhaj, M. Goueygou, A. Djerbi, M. Kaczmarek, Correlation between porosity, permeability and ultrasonic parameters of mortar with variable water/cement ratio and water content, Cement Concr. Res. 36 (2006) 625–633, https://doi.org/10.1016/j.cemconres.2005.11.009.
[44] A. Alsaif, Y.R. Alharbi, Strength, durability and shrinkage behaviours of steel fiber reinforced rubberized concrete, Construct. Build. Mater. 345 (2022) 128295, https://doi.org/10.1016/j.conbuildmat.2022.128295.
[45] N.V. Gama, A. Ferreira, A. Barros-Timmons, Polyurethane foams: past, present, and future, Materials 11 (10) (2018) 1841, https://doi.org/10.3390/ma11101841.
[46] M. Borrega, P. Ahvenainen, R. Serimaa, L. Gibson, Composition and structure of balsa (Ochroma pyramidale) wood, Wood Sci. Technol. 49 (2015) 403–420, https://doi.org/10.1007/s00226-015-0700-5.
[47] Á. Salesa, J.A. Pérez-Benedicto, D. Colorado-Aranguren, P.L. López-Julián, L.M. Esteban, L.J. Sanz-Baldúz, J.L. Sáez-Hostaled, J. Ramis, D. Olivares, Physico – mechanical properties of multi – recycled concrete from precast concrete industry, J. Clean. Prod. 141 (2017) 248–255, https://doi.org/10.1016/j.jclepro.2016.09.058.
[48] M. Bakhshi, B. Mobasher, M. Zenouzi, Model for early-age rate of evaporation of cement-based materials, J. Eng. Mech. 138 (11) (2012) 1372–1380, https://doi.org/10.1061/(asce)em.1943-7889.0000435.
[49] G. Bai, C. Zhu, C. Liu, B. Liu, An evaluation of the recycled aggregate characteristics and the recycled aggregate concrete mechanical properties, Construct. Build. Mater. 240 (2020) 117978, https://doi.org/10.1016/j.conbuildmat.2019.117978.
[50] J. Liu, F. Han, G. Cui, Q. Zhang, J. Lv, L. Zhang, Z. Yang, Combined effect of coarse aggregate and fiber on tensile behavior of ultra-high performance concrete, Construct. Build. Mater. 121 (2016) 310–318, https://doi.org/10.1016/j.conbuildmat.2016.05.039.
[51] N. Yousefieh, A. Joshaghani, E. Hajibandeh, M. Shekarchi, Influence of fibers on drying shrinkage in restrained concrete, Construct. Build. Mater. 148 (2017) 833–845, https://doi.org/10.1016/j.conbuildmat.2017.05.093.
[52] R.V. Silva, J. De Brito, R.K. Dhir, The influence of the use of recycled aggregates on the compressive strength of concrete: a review, Eur. J. Environ. Civ. Eng. 19 (2015) 825–849, https://doi.org/10.1080/19648189.2014.974831.
[53] A. Al-Mansour, S. Chen, C. Xu, Y. Peng, J. Wang, S. Ruan, Q. Zeng, Sustainable cement mortar with recycled plastics enabled by the matrix-aggregate compatibility improvement, Construct. Build. Mater. 318 (2022) 125994, https://doi.org/10.1016/j.conbuildmat.2021.125994.
[54] J. Ahmad, R.A. González-Lezcano, A. Majdi, N. Ben Kahla, A.F. Deifalla, M.A. El-Shorbagy, Glass fibers reinforced concrete: overview on mechanical, durability and microstructure analysis, Materials 15 (15) (2022) 5111, https://doi.org/10.3390/ma15155111.
[55] W. He, X. Kong, Y. Fu, C. Zhou, Z. Zheng, Experimental investigation on the mechanical properties and microstructure of hybrid fiber reinforced recycled aggregate concrete, Construct. Build. Mater. 261 (2020) 120488, https://doi.org/10.1016/j.conbuildmat.2020.120488.
[56] A.A. Ramezanianpour, V.M. Malhotra, Effect of curing on the compressive strength, resistance to chloride-ion penetration and porosity of concretes incorporating slag, fly ash or silica fume, Cem. Concr. Compos. 17 (1995) 125–133, https://doi.org/10.1016/0958-9465(95)00005-W.

[57] F. López Gayarre, C. López-Colina Pérez, M.A. Serrano López, A. Domingo Cabo, The effect of curing conditions on the compressive strength of recycled aggregate concrete, Construct. Build. Mater. 53 (2014) 260–266, https://doi.org/10.1016/j.conbuildmat.2013.11.112.
[58] S. Seara-Paz, B. González-Fonteboa, F. Martínez-Abella, J. Eiras-López, Flexural performance of reinforced concrete beams made with recycled concrete coarse aggregate, Eng. Struct. 156 (2018) 32–45, https://doi.org/10.1016/j.engstruct.2017.11.015.
[59] J. García-González, D. Rodríguez-Robles, J. Wang, N. De Belie, J.M. Morán-del Pozo, M.I. Guerra-Romero, A. Juan-Valdés, Quality improvement of mixed and ceramic recycled aggregates by biodeposition of calcium carbonate, Construct. Build. Mater. 154 (2017) 1015–1023, https://doi.org/10.1016/j.conbuildmat.2017.08.039.
[60] G.T. Xu, M.J. Liu, Y. Xiang, B. Fu, Valorization of macro fibers recycled from decommissioned turbine blades as discrete reinforcement in concrete, J. Clean. Prod. 379 (2022) 134550, https://doi.org/10.1016/j.jclepro.2022.134550.
[61] H. Rodin, S. Nassiri, K. Englund, O. Fakron, H. Li, Recycled glass fiber reinforced polymer composites incorporated in mortar for improved mechanical performance, Construct. Build. Mater. 187 (2018) 738–751, https://doi.org/10.1016/j.conbuildmat.2018.07.169.
[62] F. Golestaneh, I. Kazemi, Cross-section asymptotic for random-effects panel data models with autoregressive errors, Commun. Stat. Simulat. Comput. (2022), https://doi.org/10.1080/03610918.2022.2154799.
[63] Government of Extremadura, Construction Prices Guide, 2023 (in Spanish).